Growth of Pt−Rh Alloy Crystallites on α-Al_2O_3 Studied by Atomic Force Microscopy and Rutherford Backscattering Spectroscopy

Kohei Okumura,* Shi-aki Hyodo, and Shoji Noda

Toyota Central Research and Development Laboratories, Inc., Nagakute, Aichi 480-1192, Japan

Yusei Maruyama[†]

Institute for Molecular Science, Myodaiji, Okazaki 444-8585, Japan

Received: October 22, 1997; In Final Form: January 27, 1998

The growth of Pt−Rh alloy crystallites vacuum-deposited on α-Al_2O_3 substrates by thermal treatment was investigated by atomic force microscopy (AFM) as a function of Rh concentrations. As-deposited Pt thin film without any Rh concentration changed into Pt crystallites dispersed on the substrate by annealing at 800 °C in oxidative and reductive atmospheres. The oxidative atmosphere remarkably enhanced the growth of Pt crystallites, while it is not the case in the growth of pure Rh crystallites. However, when Rh was added to Pt, the crystallites remained very small and highly dispersed on the substrates even after the annealing at 800 °C in an oxidative atmosphere. We also investigated the surface concentration of Pt and Rh by Rutherford backscattering spectroscopy (RBS) and discussed the effect of wettability of Rh oxide as a key role in inhibiting the growth of Pt−Rh crystallites.

Introduction

The growth of metal particles was extensively investigated as one of the serious problems that decreases the activity of supported catalysts in the 1970s. Some possible growth mechanisms, the conditions where those mechanisms hold, and the desirable processes of experimental investigation have been proposed.[1−5] The general understanding of the growth of supported metal particles seems to be well-established.[6−16] However, the particular problems on supported metal particles, such as the segregation of particular elements on the surface of metal alloy particles, remained to be investigated for practical application. A detailed understanding of the behavior of catalyst components in engine exhaust gas atmosphere is important for the practical catalyst design, such as the alloy composition or the density of supported metals.

The three-way catalyst is a common base of the catalyst for automobile emission control because of the utilization of the ideal oxidation−reduction reaction of the exhaust gas molecules around the stoichiometric composition of fuel and air for complete combustion. The typical three-way catalysts contain Pt and Rh crystallites as active species.[17,18] Pt is effective for the oxidation of carbon monoxide and hydrocarbons, while Rh is effective for the reduction of nitric oxide under complicated exhaust gas conditions. To obtain the high surface area of the supported catalysts, γ-Al_2O_3 is used as a support material for the typical three-way catalysts. Although the growth of Pt crystallites on γ-Al_2O_3 and that of Rh crystallites on γ-Al_2O_3 have been studied in detail,[6−10,16] that of Pt−Rh bimetallic crystallites on γ-Al_2O_3 was less investigated.[14] To develop a method to control the growth of the metal particles for the three-way catalyst, the behavior of Pt−Rh on γ-Al_2O_3 systems should be investigated in more detail.

The previous studies of the growth of supported metal particles were mainly investigated by X-ray diffraction (XRD) and selective chemisorption with highly porous supports.[6−8] In those studies, however, the multiple origins may work on the change of metal particles' dispersion. The impossibility of determining the essential origin of the observed behaviors was pointed out.[7] Wynblatt[3] mentioned that the basic understanding of growth mechanisms in supported metal particles is likely to be accelerated by transmission electron microscopy (TEM) observation of flat model catalysts. However, the TEM observation needs skill in sample preparation and is always accompanied by the possibilities of the unexpected effect of electron beam on the observed samples. Atomic force microscopy (AFM) is free from these disadvantages of TEM observation. The sample observed with AFM can be, therefore, easily supplied for other experimental observations.[19,20]

In the present study, the growth of bimetallic Pt−Rh crystallites on a single-crystal α-Al_2O_3 (sapphire; the stable phase of Al_2O_3[21]) support with a flat surface was observed by AFM, although practical three-way catalysts adopt γ-Al_2O_3 as support material. The results of a study comparable with the present one using a flat γ-Al_2O_3 substrate as a support will be reported separately in the near future. The dependence of Pt−Rh concentration on growth behavior of the system was studied under oxidative and reductive atmospheres. Since AFM has no power to distinguish elements,[22] Rutherford backscattering spectroscopy (RBS)[23] analysis was also performed.

Experimental Section

The support used was a mirror-polished α-Al_2O_3 (sapphire) substrate with ⟨0001⟩ orientation. The planar α-Al_2O_3 substrate was chosen because it has a negligible quantity of roughness as compared with the size of the supported metal. To wash

* Corresponding author. E-mail okumura@mosk.tytlabs.co.jp, Fax +81-561-63-6150.

[†] Present address: Department of Materials Chemistry, Hosei University, Kajino, Koganei, Tokyo 184-0002, Japan.

S1089-5647(97)03409-3 CCC: $15.00
Published on Web 03/10/1998

away metal ions and the contamination layer from the surface, the substrate was boiled for 15 min in a mixture of H_2SO_4 and H_2O_2 solution with a ratio of 4 to 1.

Pt, Rh, and bimetallic Pt−Rh crystallites were fabricated by radio-frequency sputtering of Pt and Rh targets, followed by heating under a controlled atmosphere. The vacuum chamber was pumped down to 1×10^{-4} N m^{-2}, and Ar gas was introduced to 2×10^{-1} N m^{-2} to maintain the sputtering plasma. Pt or Rh was deposited up to 5 nm in thickness on the α-Al_2O_3 substrate. As for bimetallic films, Pt and Rh films were deposited alternately 10 times up to 5 nm on the α-Al_2O_3 substrate. Here, different bimetallic compositions were attained by changing the thickness of Pt and Rh films. To make these as-deposited metal films into islands, the samples were annealed under 7.5% O_2 in N_2 or 5.0% H_2 in N_2 gas flow at 800 °C for 3 h.

AFM measurement was performed using a Nanoscope E (Digital Instruments, Inc.). The AFM image was obtained in air under the constant-force mode. Each scan profile produces 512×512 data points on a total scan size of 2000×2000 nm^2. The AFM probes used were silicon nitride cantilevers having a quadrangular pyramidal tip with a cone angle of 70° and a radius of 10 nm. In some cases, these tips lead to images dominated by tip artifacts on a nanometer scale.[24,25] While we applied no correction of the tip shape to the AFM images in the following data, the grain sizes of supported metal were analyzed in consideration of the tip artifacts as later described.

The RBS measurement was performed using a 1.5 MeV He^+ beam from a 3 MeV Van de Graaff accelerator.[26] The sample was tilted about 5° from the incident beam axis to obtain definite random spectra. The detector was aligned at the scattering angle of 135°. From these data, the depth profile of the supported metal on the substrate can be calculated using a simulation program developed by Kido and Koshikawa.[27]

Results

Morphology of Supported Metal Measured by AFM. Figures 1 and 2 display AFM images of Pt/α-Al_2O_3, Rh/α-Al_2O_3, and Pt−Rh/α-Al_2O_3 after annealing in oxidative and reductive atmospheres, respectively. While the sample before annealing shows a flat surface similar to that of the α-Al_2O_3 substrates, the sample after annealing shows metal islands dispersing on the α-Al_2O_3 surface.

Pt/α-Al_2O_3 annealed in an oxidative atmosphere shows the growth of Pt crystallites from the initially deposited film to sizes ranging from 50 to 200 nm (Figure 1a). The average thickness of the particles is about 10 nm, and the value is much greater than that of the initial Pt films. The top views of most grown Pt crystallites are polygonal; especially, hexagonal or six-sided outlines predominate. These hexagonally shaped Pt crystallites have (111) preferred orientation according to XRD analysis. The previously reported TEM experiments on model Pt/SiO_2 catalysts also showed similar Pt crystallites with (111) preferred orientation.[11,15]

For the bimetallic films on α-Al_2O_3 after annealing in an oxidative atmosphere, the surface morphology was completely different from that of Pt/α-Al_2O_3. Even a small quantity of Rh additive causes a drastic change in the metal particle shape; that is, necked islands (Figure 1b) and meshlike islands (Figure 1c) are observed. The growth of metal particles came to be much more reduced with increasing Rh (Figure 1d−f). The image obtained for the sample that contains only Rh shows fairly small particles (Figure 1g). Since the average vertical distance between peaks and valleys is below 1 nm and is smaller than the thickness of the initial Rh film in this image, the α-Al_2O_3 substrate is still covered by Rh. The morphologies we observed here are quite similar to those previously observed by TEM for the model Rh/SiO_2 catalyst.[13]

On the other hand, when Pt−Rh/α-Al_2O_3 was annealed in a reductive atmosphere, the metal particles remarkably grew even if Rh was loaded (Figure 2). The average particle sizes are about 100 nm in all the Pt−Rh/α-Al_2O_3 samples. The shape of the metal particles grown in a reductive atmosphere is roughly hemispherical or hexagonal and is rather different from that of Pt crystallites grown in an oxidative atmosphere shown in Figure 1a. Wang et al. have previously investigated the effect of gas treatment on the shape of Pt and Rh crystallites supported on planar SiO_2 and γ-Al_2O_3 by using TEM. They found that growth of Pt on SiO_2 or γ-Al_2O_3 yields predominantly (100) oriented particles with a square outline under reductive atmospheres.[15] However, as shown in Figure 2a, Pt metals grown on α-Al_2O_3 crystallize, forming facets with various shapes. They were identified as Pt crystallites of (111) orientation and Pt_8-Al_{21} compounds by XRD experiments. Such intermetallic compounds have been also observed on Pt/α-Al_2O_3 by Chu et al.[9]

Figure 3 shows the effect of Rh loading on the coverage of metal particles on α-Al_2O_3 substrate. To obtain correct coverage values, the influence of the tip geometry is subtracted from the row AFM data. The artifact of the tip geometry comes from the fact that the contact point between the tip and the particle is not only the apex of the tip but also its side wall when the AFM tip is scanned over a particle on a flat substrate.[24,25] The coverage shown in Figure 3 is the corrected values referring to a tip radius of 10 nm. The coverage obtained for Pt/α-Al_2O_3 after the annealing in an oxidative and a reductive atmosphere is about 40% and 20%, respectively. The value of the coverage increases slightly with increasing Rh for the sample annealed in a reductive atmosphere. In an oxidative atmosphere, the coverage decreases with increasing Rh until 10% loading. Above the 10% Rh loading, the coverage rapidly increases and saturates at about 50% Rh loading. This rapidly increasing region corresponds to the typical Pt−Rh composition of the practical three-way catalysts.[17] It seems that this range of Rh loading is quite meaningful for the inhibition of the growth of Pt crystallites.

Surface Composition of Supported Metal Measured by RBS. Figure 4 shows the RBS spectra for the samples whose morphologies were shown in Figures 1 and 2. In this figure, only the spectrum portion corresponding to Pt and Rh is displayed. The average thickness of metal films or the height of the islands was obtained by the spectral shape simulations[27] using the atomic density of Pt and Rh.

For all samples before annealing, intense peaks appear in the spectra (solid lines in Figure 4). The average thickness of the metal films estimated from the peak width is about 35 nm, which is much greater than the nominal deposition thickness (5 nm). This is because the energy resolution of our RBS apparatus is about 20 keV. This energy resolution corresponds to the depth resolution of 25−30 nm for Pt or Rh.

For Pt/α-Al_2O_3 samples shown in Figure 4a, the remarkable broadening of the Pt peaks was observed after both oxidative and reductive annealing. In addition, in the spectrum portion of much lower energy not indicated here, the energy values corresponding to the Al and O surface slightly shift to higher energy. These results indicate a morphological change in the Pt layer from a plane film into islands, exposing the α-Al_2O_3 substrate surface. The total backscattering yield of the Pt peak

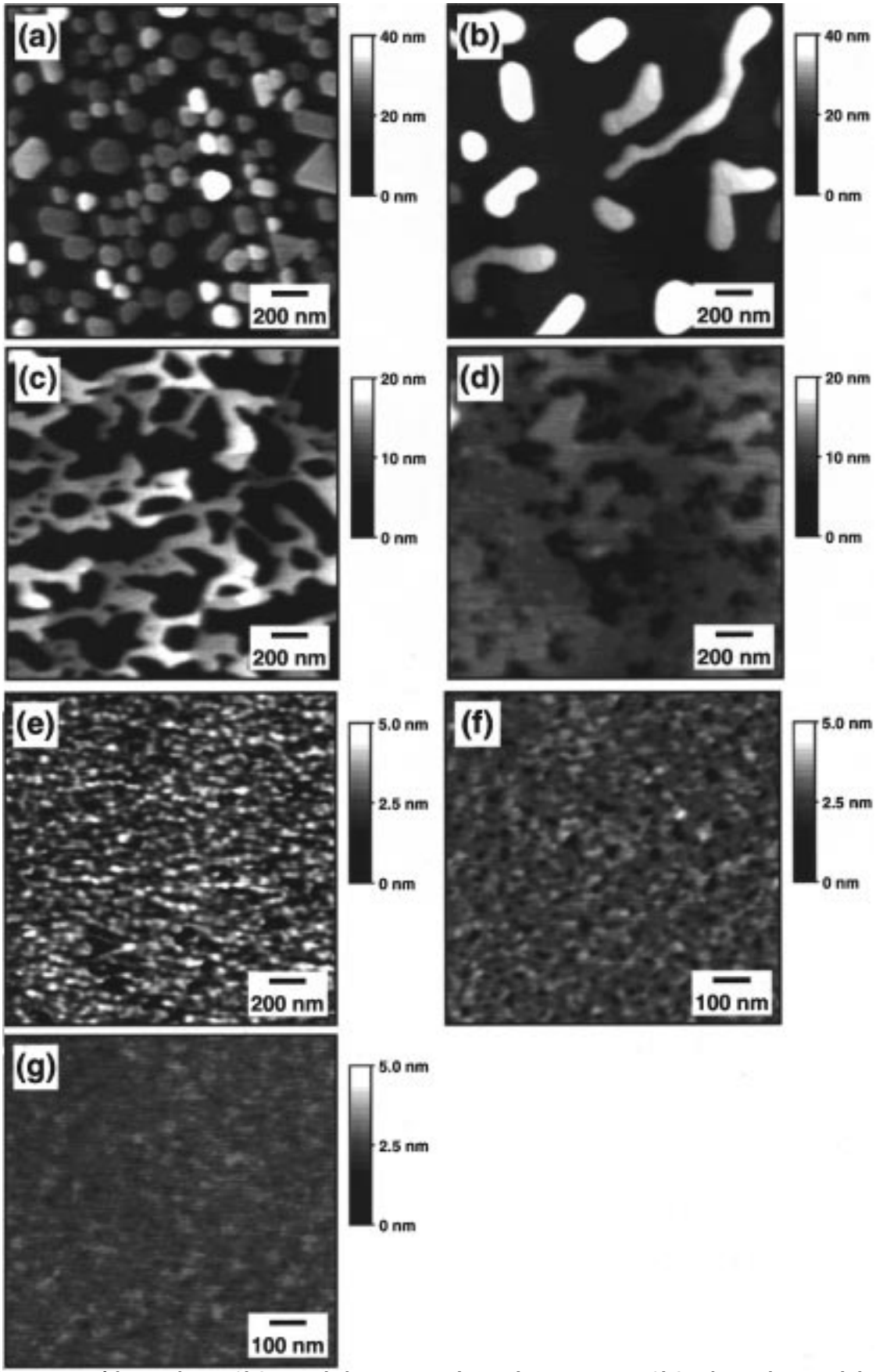

Figure 1. AFM images of the Pt−Rh on α-Al_2O_3. Pt and Rh were sputter-deposited up to 5 nm on α-Al_2O_3 substrate then annealed at 800 °C for 3 h under 7.5% O_2 in N_2 atmosphere. The mixing ratio of Pt to Rh was (a) 10 to 0, (b) 9 to 1, (c) 8 to 2, (d) 6 to 4, (e) 4 to 6, (f) 2 to 8, and (g) 0 to 10.

for annealed samples is almost equal to that of the one before annealing, indicating no loss of Pt from α-Al_2O_3 substrate surface. The average thicknesses of the Pt islands for the samples after oxidative and reductive treatments are derived to

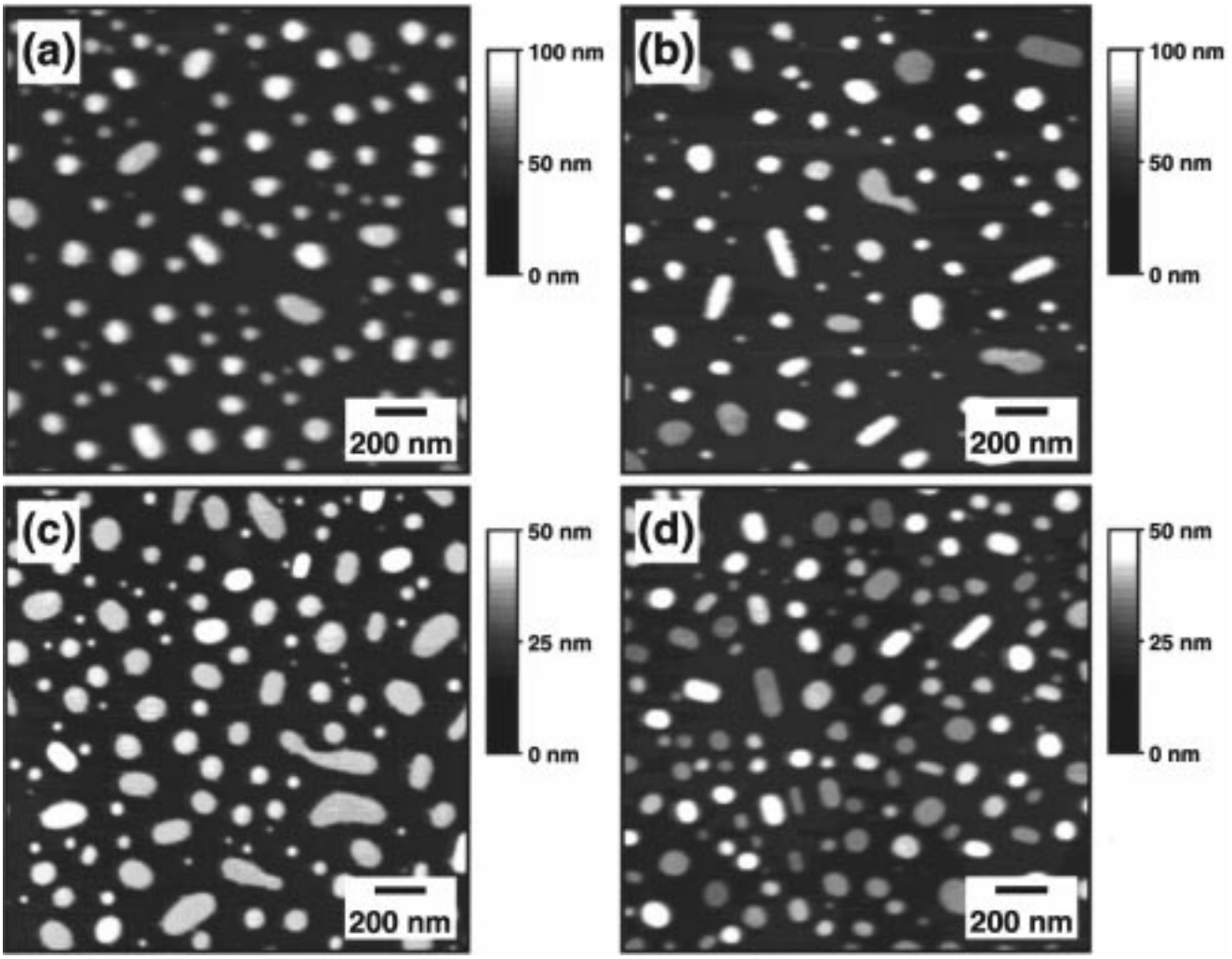

Figure 2. AFM images of the Pt−Rh on α-Al_2O_3. Pt and Rh were sputter-deposited up to 5 nm on α-Al_2O_3 substrate then annealed at 800 °C for 3 h under 5.0% H_2 in N_2 atmosphere. The mixing ratio of Pt to Rh was (a) 10 to 0, (b) 8 to 2, (c) 5 to 5, and (d) 0 to 10.

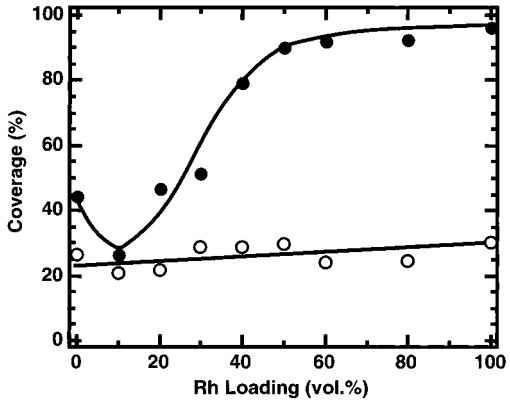

Figure 3. Effect of Rh loading on the coverage of metal on the α-Al_2O_3. The Pt−Rh were sputter-deposited up to 5 nm in thickness on α-Al_2O_3 substrate then annealed at 800 °C for 3 h under 7.5% O_2 in N_2 (closed circle) and under 5.0% H_2 in N_2 (open circle) atmosphere.

be 18 and 37 nm, respectively, after subtracting the influence of the depth resolution. These values are consistent with the values obtained by AFM measurement.

For Rh/α-Al_2O_3 shown in Figure 4b, the remarkable broadening of the Rh peak was observed only for the sample after a reductive annealing. The thickness of Rh layer is estimated to be 29 nm. After an oxidative annealing, the Rh peak still maintains sharpness, indicating 5 nm in thickness. The energy values corresponding to the Al and O surface do not shift from the initial energy values. The formation of Rh oxide is confirmed by X-ray photoelectron spectroscopy (XPS). Therefore, the Rh oxide is considered to remain as a film or extremely small islands.

For Pt−Rh/α-Al_2O_3 shown in Figure 4c, the remarkable broadening of the Pt and Rh peaks was observed only for after a reductive annealing just as the Rh/α-Al_2O_3 sample. After a reductive annealing, the Pt and Rh peak heights showed 40% decrease, and the thickness is 21−22 nm. After an oxidative annealing, the Pt and Rh peak heights showed 20% decrease. The average thicknesses of the metal islands slightly increase to 5−7 nm. Taking the similar thickness values for Pt and Rh into consideration, both metal species have grown from plane films to islands as a mixture or an alloy during annealing. If Pt and Rh had grown independently, the Pt and Rh peaks might have broadened differently as shown in Figure 4a,b.

Discussion

The growth mechanism of supported Pt has been widely investigated, and several growth models have been proposed.[1−5] Wynblatt et al. have reported that volatile PtO_2 transfers from small Pt crystallites to large ones through the vapor phase in an oxidative atmosphere at high temperature.[2,3] In accordance with this, Pt crystallites grew remarkably in an oxidative atmosphere in our experiment as shown in Figure 1a. However,

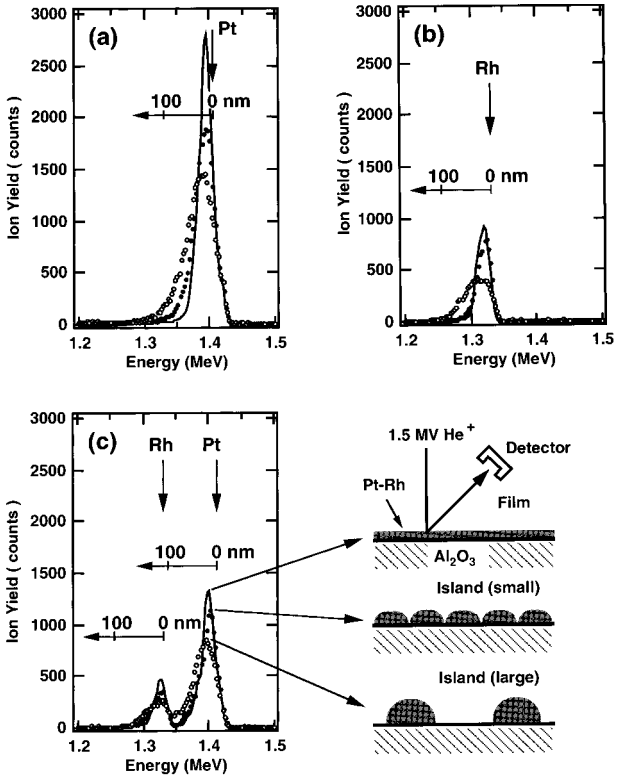

Figure 4. RBS spectra from the (a) Pt on α-Al_2O_3, (b) Rh on α-Al_2O_3, and (c) Pt−50% Rh on α-Al_2O_3 and schematic illustration of island structure. The solid curve denotes the spectra from the as-deposited metal film on the α-Al_2O_3 substrate. The closed and open circles denote the spectra from the metal islands on the α-Al_2O_3 substrate after annealing at 800 °C for 3 h under 7.5% O_2 in N_2 and under 5.0% H_2 in N_2 atmosphere, respectively. The surface positions of Pt and Rh are indicated by arrows. The scales are inserted for the thickness of the plane films or islands.

considerable growth was also observed in samples treated in a reductive atmosphere (Figure 2a). This suggests that there exists an another growth process such as coalescence of particles or interparticle Pt transfer by surface diffusion. Chen et al. have suggested the existence of the surface diffusion process in the Pt/SiO_2 system.[11]

For Rh/α-Al_2O_3, the growth of metal particles is inhibited in an oxidative atmosphere (Figure 1g), while Rh grew remarkably in a reductive atmosphere (Figure 2d). There have been some reports concerning the effect of oxidizing environments on the behavior of Al_2O_3-supported Rh using the temperature-programmed reduction (TPR) method.[8,28] It is reported that the Rh oxide strongly interacts with the γ-Al_2O_3 above 600 °C.[8] In our experiment, Rh oxide is found by XPS on both Rh/α-Al_2O_3 and Pt−Rh/α-Al_2O_3 after oxidative heat treatment. The XPS peak of Rh $3d_{5/2}$ appeared around 309 eV, being very close to that of Rh_2O_3: 308.7 eV.[29] Rh_2O_3 is quite stable up to 1000 °C, while PtO_2 is decomposed into Pt and O_2 above 550 °C even under oxidative conditions.[13,30] Generally metal oxides tend to wet supports better than pure metals.[10] Therefore, the inhibition of the growth of Rh crystallites in an oxidative atmosphere can be attributed to the wettability of surface Rh oxide with Al_2O_3. This good wettability of Rh oxide with Al_2O_3 may go so far to have Rh oxide submerge into Al_2O_3 as speculated by McCabe et al. on the basis of the indirect evidence of TPR experiments.[28] In our system, however, RBS results directly show that the Rh oxides did not go so far to submerge into bulk α-Al_2O_3 but exist on the α-Al_2O_3 surface. It should be noted that this difference might be caused by the difference in the aging condition between McCabe et al. (hydrothermal aging at 950 °C) and us (7.5% O_2 in N_2 at 800 °C).

As previously mentioned, Pt and Rh show different growth behavior during heat treatment, especially under oxidative conditions. For Pt−Rh/α-Al_2O_3, the RBS results indicate that Pt and Rh form an alloy on α-Al_2O_3 after annealing (Figure 4c), and the growth of bimetallic Pt and Rh crystallites seems to be controlled by the nature of Rh. The formation of Pt−Rh alloy has also been observed for the Pt−Rh/SiO_2 system by TEM.[13] Under oxidative conditions, a small amount of Rh drastically changes the surface morphology of Pt−Rh/α-Al_2O_3 (Figure 1a−c). The coverage of the metal for Pt−Rh/α-Al_2O_3 containing 60% Rh is almost equal to that of Rh/α-Al_2O_3 (Figures 1e−g and 3). These facts explain that the presence of Rh_2O_3 improves the wettability of bimetallic Pt−Rh alloy crystallites with the α-Al_2O_3 substrate, and simultaneously Rh_2O_3 stabilizes the bimetallic particles on α-Al_2O_3. In addition, the Rh oxide segregation has been previously reported for the Pt−Rh/SiO_2 system using electron diffraction analysis.[13] It is expected that the segregation of Rh oxide occurs in the Pt−Rh/α-Al_2O_3 system. The segregated Rh oxide is supposed to strongly stabilize the bimetallic particles on α-Al_2O_3 and inhibit the evaporation of PtO_2.

Conclusions

The growth of Pt−Rh alloy crystallites vacuum-deposited on α-Al_2O_3 substrates by thermal treatment was investigated by AFM as a function of Rh concentrations. As-deposited Pt thin film without any Rh concentration changed into Pt crystallites dispersed on the substrate by annealing at 800 °C in oxidative and reductive atmospheres. The oxidative atmosphere remarkably enhanced the growth of Pt crystallites, while it is not the case in the growth of pure Rh crystallites. However, when Rh was added to Pt, the crystallites remained very small and highly dispersed on the substrates even after the annealing at 800 °C in an oxidative atmosphere. RBS results indicated that Pt and Rh had grown from a plane film into islands with the formation of an alloy during heat treatment. The high wettability of Rh oxide for α-Al_2O_3 as well as the surface segregation of Rh oxide is supposed to contribute to the inhibition for growth of Pt crystallites.

Acknowledgment. The authors wish to thank N. Takahashi and K. Dohmae for XPS measurements and I. Konomi, A. Kawano, and T. Motohiro for their helpful suggestions and discussion.

References and Notes

(1) Granqvist, C. G.; Buhrman, R. A. *J. Appl. Phys.* **1976**, *47*, 2200.
(2) Wynblatt, P.; Gjostein, N. A. *Acta Metall.* **1976**, *24*, 1165.
(3) Wynblatt, P. *Acta Metall.* **1976**, *24*, 1175.
(4) Flynn, P. C.; Wanke, S. E. *J. Catal.* **1974**, *34*, 390.
(5) Rukenstein, E.; Pulvermacher, B. *J. Catal.* **1973**, *29*, 224.
(6) Fiedorow, R. M. J.; Wanke, S. E. *J. Catal.* **1976**, *43*, 34.
(7) Fiedorow, R. M. J.; Chahar, B. S.; Wanke, S. E. *J. Catal.* **1978**, *51*, 193.
(8) Yao, H. C.; Japar, S.; Shelef, M. *J. Catal.* **1977**, *50*, 407.
(9) Chu, Y. F.; Ruckenstein, E. *J. Catal.* **1978**, *55*, 281.
(10) Ruckenstein, E.; Chu, Y. F. *J. Catal.* **1979**, *59*, 109.
(11) Chen, M.; Schmidt, L. D. *J. Catal.* **1978**, *55*, 348.
(12) Chen, M.; Schmidt, L. D. *J. Catal.* **1979**, *56*, 198.
(13) Chen, M.; Wang, J.; Schmidt, L. D. *J. Catal.* **1979**, *60*, 356.
(14) Wang, T.; Schmidt, L. D. *J. Catal.* **1981**, *70*, 187.
(15) Wang, T.; Lee, C.; Schmidt, L. D. *Surf. Sci.* **1985**, *163*, 181.
(16) Harris, P. J. F.; Boyes, E. D.; Cairns, J. A. *J. Catal.* **1983**, *82*, 127.
(17) Kummer, J. T. *Prog. Energy Combust. Sci.* **1980**, *6*, 177.

(18) Herz, R. K.; Shinouskis, E. J.; Datye, A.; Schwank, J. *Ind. Eng. Chem. Prod. Res. Dev.* **1985**, *24*, 6.
(19) Erlandsson, R.; Eriksson, M.; Olsson, L.; Helmersson, U.; Lundström, I.; Petersson, L.-G. *J. Vac. Sci. Technol.* **1991**, *B9*, 825.
(20) Lee, K. H.; Wolf, E. E. *Catal. Lett.* **1994**, *26*, 297.
(21) Stiles, A. B., Ed. *Catalyst Supports and Supported Catalysts;* Butterworths: Boston, MA, 1987.
(22) Binnig, G.; Quate, C. F.; Gerber, Ch. *Phys. Rev. Lett.* **1986**, *56*, 930.
(23) Chu, W. K.; Mayer, J. W.; Nicolet, M. A. *Backscattering Spectrometry;* Academic Press: New York, 1977.
(24) Grütter, P.; Zimmermann-Edling, W.; Brodbeck, D. *Appl. Phys. Lett.* **1992**, *60*, 2741.
(25) Markiewicz, P.; Goh, C. *Langmuir* **1994**, *10*, 5.
(26) Kido, Y.; Kakeno, M.; Yamada, K.; Kawamoto, J.; Ohsawa, H.; Kawakami, T. *J. Appl. Phys.* **1985**, *58*, 3044.
(27) Kido, Y.; Koshikawa, T. *J. Appl. Phys.* **1990**, *67*, 187.
(28) McCabe, R. W.; Usmen, R. K.; Ober, K.; Gandhi, H. S. *J. Catal.* **1995**, *151*, 385.
(29) Chastain, J., Ed. *Handbook of X-ray Photoelectron Spectroscopy;* Perkin-Elmer: Eden, Prairie, MN, 1992.
(30) Berry, R. J. *Surf. Sci.* **1978**, *76*, 415.